Purdue University
Purdue e-Pubs

International Compressor Engineering Conference | School of Mechanical Engineering

1988

Development of High Efficiency Scroll Compressors, for Air Conditioners

Takahisa Hirano
Mitsubishi Heavy Industries

Noriaki Matsumura
Mitsubishi Heavy Industries

Kimiharu Takeda
Mitsubishi Heavy Industries

Follow this and additional works at: https://docs.lib.purdue.edu/icec

Hirano, Takahisa; Matsumura, Noriaki; and Takeda, Kimiharu, "Development of High Efficiency Scroll Compressors, for Air Conditioners" (1988). *International Compressor Engineering Conference.* Paper 603.
https://docs.lib.purdue.edu/icec/603

This document has been made available through Purdue e-Pubs, a service of the Purdue University Libraries. Please contact epubs@purdue.edu for additional information.
Complete proceedings may be acquired in print and on CD-ROM directly from the Ray W. Herrick Laboratories at https://engineering.purdue.edu/Herrick/Events/orderlit.html

DEVELOPMENT OF HIGH EFFICIENCY SCROLL COMPRESSORS FOR AIR CONDITIONERS

TAKAHISA HIRANO, NORIAKI MATSUMURA
NAGOYA RESEARCH & DEVELOPMENT CENTER
MITSUBISHI HEAVY INDUSTRIES, LTD., NAGOYA, JAPAN

KIMIHARU TAKEDA
AIR-CONDITIONING & REFRIGERATION MACHINERY WORKS
MITSUBISHI HEAVY INDUSTRIES, LTD., AICHI, JAPAN

ABSTRACT

Recently, a scroll compressor for air conditioners has been developed, because of its high efficiency, quiet operation, light weight and small size. To accomplish high efficiency, self sealing mechanisms such as a tip seal and a swing link mechanism are very effective. Tip seals which are placed on the top of scroll wraps achieve thrust sealing and a swing link mechanism achieves radial sealing for compressed gas leakage.

M.H.I. has been studying and developed high efficiency hermetic scroll compressors with tip seals and swing link mechanism.

This paper presents as follows.

(1) Experimental and computer simulation loss analysis (P-V diagram) were taken on wide speed range. Measured and calculated results were good agreement.
(2) Orbiting scroll motion, tip seal motion and pressure distribution in seal groove were measured. Swing link motion was measured, too. As a result, it was comfirmed that self sealing for thrust and radial clearance were accomplished well.

INTRODUCTION

As for the recent heat pump air conditioners, compressors are required to operate in a wide speed range by means of inverter drive and in a wide operating pressure range. From the points of high efficiency, high reliability and the others, scroll compressors have been used.

It is necessary to make a loss analysis in order to accomplish high efficiency of com-

pressors, however, the result of the experimental loss analysis of scroll compressor has not been reported yet.

On the other hand, it is said that a swing link mechanism and tip seals are effective for preventing the gas leakage from compression pockets, however, reports on the clarification of these behavior have apparently not been published to date.

M.H.I. has developed high efficient scroll compressors. In this paper, we describe the experimental and theorytical results of loss analysis, and measurements of the behavior of the swing link and the tip seal, that were performed in the development.

COMPRESSOR CONSTRUCTION

The construction of M.H.I.'s scroll compressor is shown in Fig. 1. The low side shell has been adopted by reason of reliability mainly. For compression pockets, tip seals have been adopted for effective thrust sealing, and the swing link mechanism for effective radial sealing.

Gas which was inhaled from the periphery of scroll is compressed in the compression pockets and is exhausted into the discharge cavity, which is designed for noise reduction, through the discharge port with a check valve.

For the purpose of bypass capacity control, unload valves are installed midway of the compression pockets, and the capacity control can be carried out by opening and closing the valves.

In order to obtain the high reliable compressor, a special journal bearing is used for the drive bearing which drives the orbiting scroll, a roller bearing for the main bearing, an aluminum metal for the lower bearing and a special shaped thrust bearing.

LOSS ANALYSIS

As for loss analysis, there are two methods, one is an experimental method drawing up a P-V diagram on the basis of the cylinder pressure, and the other is an analytical method carrying out a performance simulation. We performed loss analysis using both methods under various speed and pressure conditions by inverter drive.

(1) Measurement of P-V diagram

M.H.I.'s scroll compressor has its compression and discharge process extending to a range of about 920°. In order to measure pressures of all the compression pockets which are formed approximately bisymmetrically at the same time, we mounted seven piezo-electric pressure sensors in the fixed scroll considering the detecting overlap angles of the pressure sensors. Three of them P_5, P_3 and P_1 are in the pockets at the outer curve of the fixed scroll, three of them P_6, P_4 and P_2 are in the pockets at the inner curve of the fixed scroll, and one of them P_0 is at the discharge port. And we carried out the measurements in the same way as shown in the reference.[1)]

In Fig. 2, cylinder pressure diagram (P-θ) and P-V diagram are shown. Here, pressures in the inner curve pockets, P_4 and P_2, are a little higher than pressures in the outer

curve pockets of the fixed scroll, P_3 and P_1. The gas leakage in the inner curve pockets is rather larger than that in the outer curve pockets slightly.

These relationships were observed under all measuring conditions, and it is considered that the orbiting scroll in the tested machine was counterclockwise twisted slightly.

The comparison of P-V diagrams concerning the outer curve pockets of the fixed scroll at the pressure ratios are respectively high (i.e. $\phi = 6.5$), near to the design pressure ratio (i.e. $\phi = 3.3$) and low (i.e. $\phi = 2.6$) is shown in Fig. 3. Here, the design pressure ratio $\phi_i \cong$ 3.2.

In the case of the high pressure ratio, owing to the operation of the check valve, a sudden back flow from the discharge cavity to the central compression pocket does not take place and a good compression curve is obtained.

On the other hand, in the case of the low pressure ratio, the pressure in central compression pocket becomes excessively high beyond the cavity pressure before the pocket communicates with the discharge port, so attention must be paid to this over compression when designing or using the scroll compressors.

P-V diagrams when the operating frequency is changed from 45 to 105 Hz are shown in Fig. 4. When the speed is low, the influence due to the leakage of compression pockets can be observed.

As the speed is increased, the leakage is reduced, however, the overshoot in discharge process is enlarged. To perform a high speed operation, it is needed to pay attention to the reduction of the discharge wire drawing.

(2) Performance Simulation

The detailed discussion of the performance simulation will be separately reported, so the details are omitted in this paper.

The particular features of M.H.I.'s performance simulation are as follows:

1) Three leakage passages as shown in Fig. 5 are considered.
   (Mesh clearance, tip clearance and bypass pathway by the side of and at the lower part of tip seal)
2) Both compression pockets which are formed bisymmetrically are included in the calculation independently each other.
3) The fact that the orbiting scroll goes across the discharge port is considered.

P-V diagram obtained by the performance simulation is shown in Fig. 6.

Close agreement between Fig. 2-2 and Fig. 6 is obtained, and the propriety of the performance simulation is confirmed.

(3) Loss Analysis

The measured values and the results of loss analysis by performance simulation are shown in Fig. 7.

As for EER and various efficiencies (various losses), their experimental values agree well with calculation results over wide speed range.

As the rotational speed is increased, EER is decreased. This is due to the decreasing of indicated efficiency (the increasing of indicated loss).

The indicated loss can be analyzed into gas leakage, superheating of suction gas, pressure drops of suction and discharge lines, and wire drawing. The decreasing of indicated efficiency at the high speed is caused principally by the increasing of the discharge wire drawing.

It was confirmed that the leakage is few owing to a good sealing of the compression pockets by means of the tip seals and the swing link mechanism which are described later, and that the pressure drop due to discharge cavity is small.

In order to obtain high EER at the high speed, the discharge porting is an important item for decreasing discharge wire drawing.

MEASUREMENT OF SWING LINK MOTION

The analysis of the swing link mechanism was shown in report,[2] and here, we measured the swing link motion.

A measuring-ring was attached to the balance weight and two eddy-current sensors were mounted in the motor case with a phase difference of 90° between the two. (Fig. 8) The measurement of the swing link motion was carried out by detecting the gap and drawing Lissajous's figure.

The symbols used in Fig. 8 are given below:

r = radius of measuring ring
Δr = distance between shaft center and ring center
lx = distance between X – axis sensor and shaft center
ly = distance between Y – axis sensor and shaft center
x = gap between X – axis sensor and ring periphery
y = gap between Y – axis sensor and ring periphery

Where the relationship of x and y is shown approximately by the following equation.

$$\{x-(lx-r)\}^2+\{y-(ly-r)\}^2=\Delta r^2$$

When the signals proportional to x and y are obtained, the change of swing radius can be obtained as a change of circle with a radius Δr.

To confirm the motion of the swing link, the special fixed scroll with a projection was made and both cases of the fixed scrolls with and without the projection were compared. The swing link motion was also confirmed under several operating conditions. These examples are shown in Fig. 9.

In both cases of operating conditions I and II, portion A shows the position corresponding to the projection, and it is found that the swing radius changes at this position.

In the case of operating condition I, fine ripples can be observed at portion B because of the errors in machinings. These fine ripples disappear after operating for about 10 hours. The reason is for that the initial wear occurs during run-in.

Furthermore the radius Δr is different in condition I and II. We can consider that the deformation of the crank pin, the bearings and the scrolls depends on operating condition and that the swing link follows the deformation.

On the other hand, the motion in starting up is shown in Fig. 10. The compressor begin to rotate and the radius of Lissajous's circle becomes suddenly small when it is turned by about 1-3/4 revolutions and thereafter the radius of Lissajous's circle becomes smaller gradually as the pressure increases. That is, both scrolls engage with each other when 1-3/4 revolutions are made, and the swing link follows the pressure deformation thereafter.

MEASUREMENTS OF TIP SEAL MOTION

The behavior of the tip seal is related to the pressure in the tip seal groove, and the orbiting scroll performs an orbiting in a tilting position. Here, we measured the pressure in the tip seal groove and the orbiting scroll posture as well as the tip seal motion.

(1) Pressure in Tip Seal Groove

Several piezo-electric pressure sensors and Bourdon tube pressure gauges were mounted in the tip seal groove of the fixed scroll, and the pressures along the spiral were measured at the same time. The results including the cylinder pressure are shown in Fig. 11. At the positions Pa and Pb near the center of spiral, a relatively higher pressure that is next to the discharge pressure is generated, while at the outside position Pc, the pressure is considerably low. The pressure distribution and the pressure fluctuation in the seal groove were clarified.

The differential pressure Ps which presses the tip seal against the opposing scroll is approximately considered as follows:

$$\text{Ps} = \text{Pressure in seal groove} - \left(\begin{matrix}\text{Cylinder pressure of} \\ \text{inside pocket}\end{matrix} + \begin{matrix}\text{Cylinder pressure of} \\ \text{outside pocket}\end{matrix}\right)/2$$

As a result of investigating the characteristic of the mean differential pressure Ps during one revolution under various operating conditions, Fig. 12 is obtained. That is, the mean differential pressure Ps can be arranged by the difference between the high pressure and the low pressure.

(2) Inclination of Orbiting Scroll

The inclination of the orbiting scroll was measured by several eddy-current sensors mounted in the thrust bearing. The results are shown in Fig. 13.

The inclination of the orbiting scroll α% is about 0.1 when it is assumed that the geometrical maximum inclination = 1.0. The angle of inclined direction γ is behind the crank

angle θ by about 120 degrees. According to our another theoretical analysis, the difference between θ and γ is 100 ~ 110 degrees, this agrees with above-mentioned results.

(3) Tip Seal Motion

The displacement of the tip seal was measured by several eddy-current sensors mounted in the tip seal groove of the fixed scroll, and the results are shown in Fig. 14.

It is found that the tip seal moves with crank angle toward the longitudinal direction in the seal groove. As the above-mentioned direction of inclination of the orbiting scroll is behind the real crank angle by 120 degrees, it is found that the orbiting scroll is tilted in the directions of mounted sensors [$\gamma = 270°$ and 90° (450°)] when crank angle $\theta = 150°$ and 330° respectively. Each displacement of the tip seal in this case is shown in Fig. 15.

The inclination obtained by the outerside sensors G_{III} and G_{IV} agrees with the inclination shown in the figure above-mentioned, while the variations of the tip seal displacement at the central portion of the scroll are much larger than those of this inclination. That is, it is found that the member of the scroll is deformed by cylinder pressure and the deformation is varied with crank angle. Also, it is confirmed the tip seal follows well the change of clearance due to cylinder pressure change. In this connection, the values of deformation which were obtained in our another analysis agree with the above-mentioned results.

CONCLUSIONS

In regard to the low side scroll compressor with swing link mechanism and tip seals, we have concluded from various measurements and analyses as follows:

(1) We carried out the measurements of cylinder pressure and loss analyses under various speed and operating conditions. Discharge porting is particularly important to reduce wire drawing.

(2) Close agreement between the above-mentioned results and the simulation was obtained. The simulation can be satisfactorily utilized as a designing tool.

(3) As a result of measuring the swing link motion, it was confirmed that the swing link followed the machining error and pressure deformation. The swing link mechanism effectively seals the mesh clearances.

(4) By measuring the pressure in the tip seal groove, the pressing pressure of the tip seal was clarified. In addition, the tilting motion of the orbiting scroll and the tip seal motion were clarified. The scroll is deformed by the cylinder pressure. The tip seal seals the fluctuating tip clearance that is due to deformation by the cylinder pressure and the inclination of the orbiting scroll excellently.

REFERENCES

1) N. Murata, M. Fujitani, "Improvement of P-V Diagram Measurements," 1984 Purdue Compressor Conference

2) K. Hagimoto, S. Hirakawa, T. Hirano, "An Analytical Study of the Kinematics of Scroll Compressor," Mitsubishi Heavy Industries Technical Review, October 1986

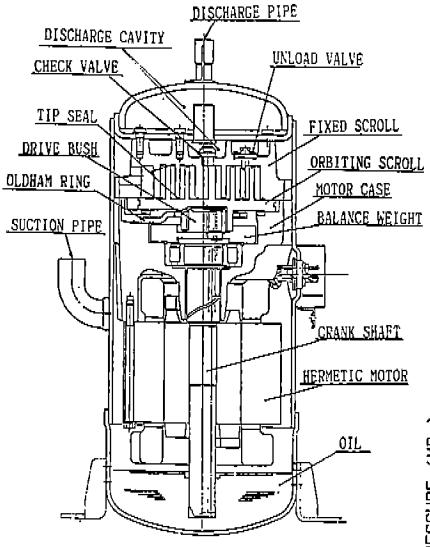

FIG.1 COMPRESSOR CONSTRUCTION

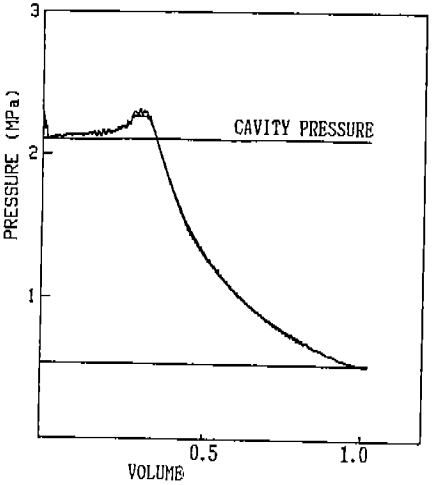

FIG.2-2 P-V DIAGRAM

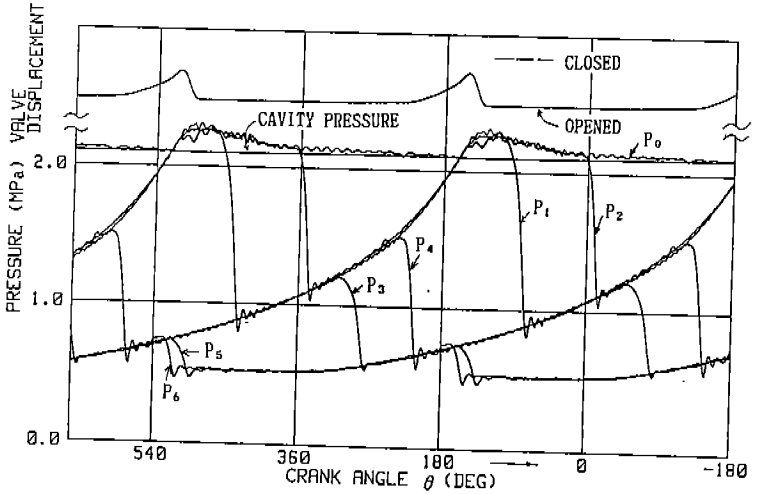

FIG.2-1 P-θ DIAGRAM

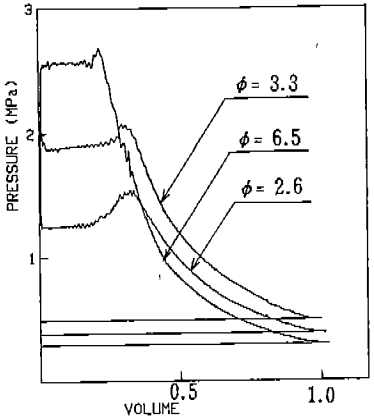

FIG.3 INFLUENCE OF PRESSURE RATIO ON P-V DIAGRAM

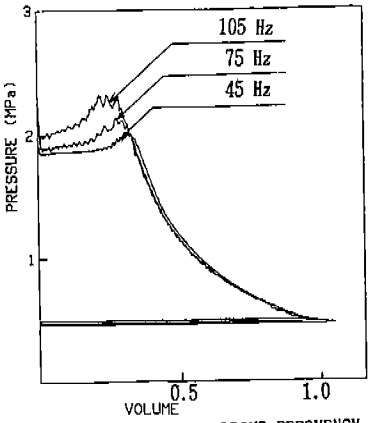

FIG.4 INFLUENCE OF DRIVE FREQUENCY ON P-V DIAGRAM

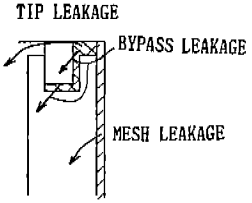

FIG 5. 3-TYPE LEAKAGE

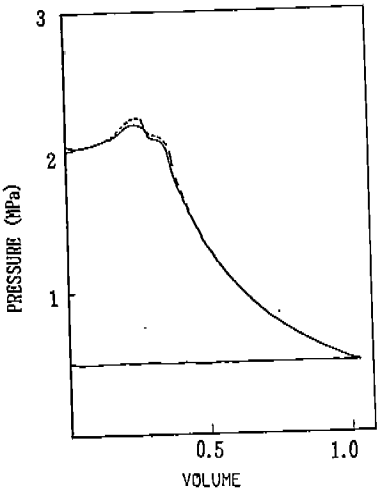

FIG.6 CALCULATED P-V DIAGRAM

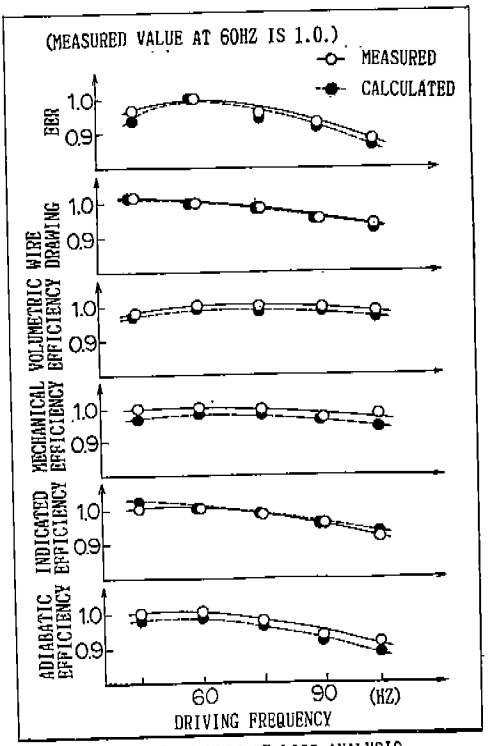

FIG.7 RESULTS OF LOSS ANALYSIS

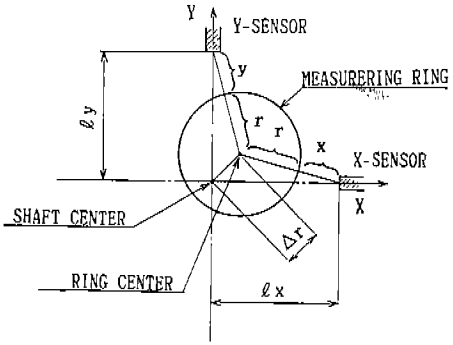

FIG.8 MEASUREMENT OF SWING LINK MOTION

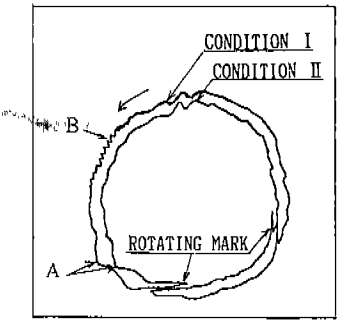

FIG.9 SWING LINK MOTION

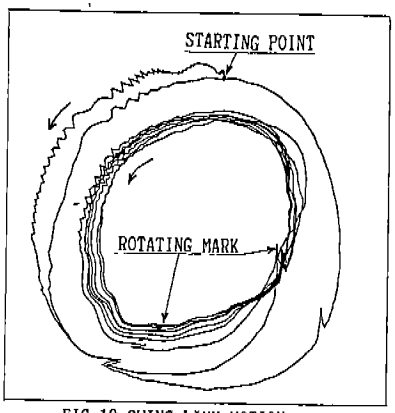

FIG.10 SWING LINK MOTION
AT STARTING UP

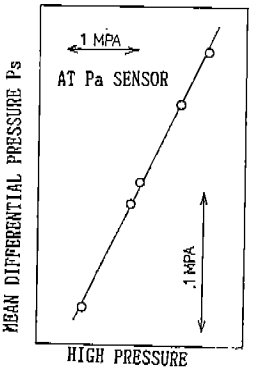

FIG.12 RELATIONSHIP BETWEEN
Ps AND OPERATING PRESSURE

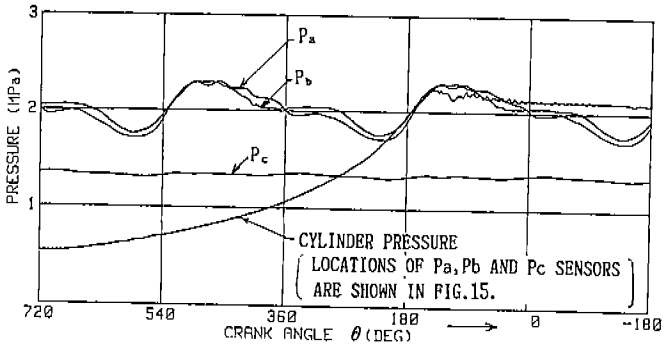

FIG.11 PRESSURES IN TIP SEAL GROOVE

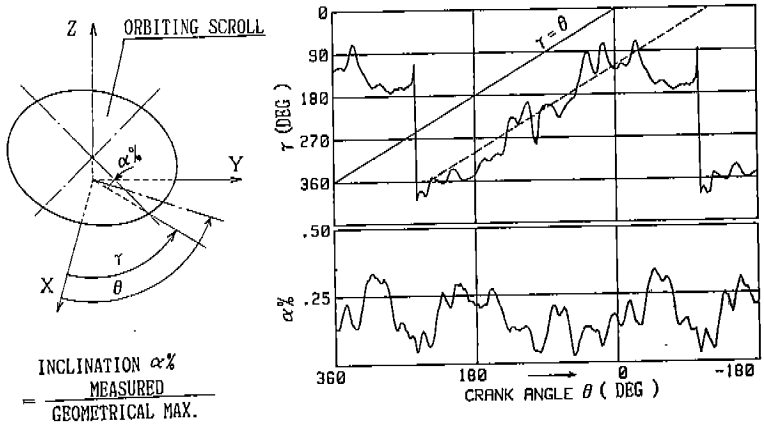

FIG.13 MOTION OF ORBITING SCROLL

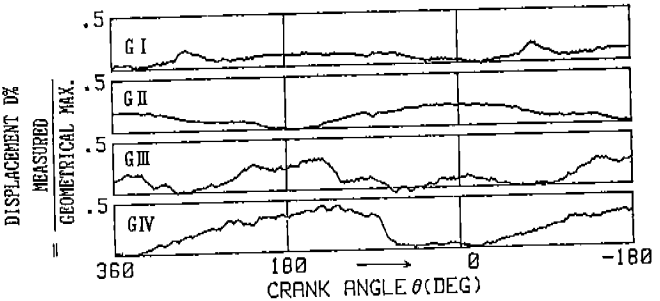

FIG.14 MOTION OF TIP SEAL

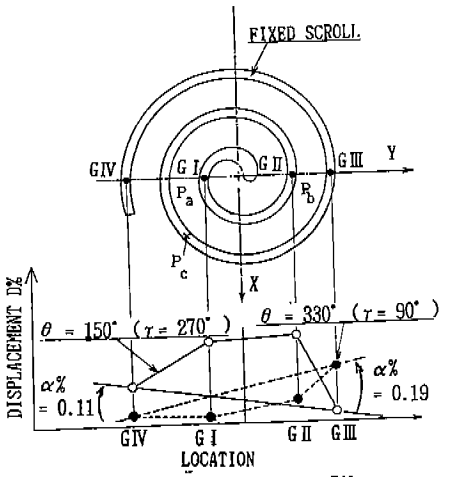

FIG.15 DISPLACEMENT OF TIP SEAL